TABLE OF CONTENTS MAIN PAGE

CH-99-11-2

A Preliminary Experimental Assessment of the Comparative Thermal Performance of Attics and Cathedral Ceilings in a Cold Climate

Louis F. Goldberg, Ph.D. **Patrick H. Huelman** **Barry B. Bridges, P.E.**
Member ASHRAE

ABSTRACT

This paper describes a residential research facility built for the experimental measurement of the relative energy and moisture performance of various residential building envelope components and systems. The building comprises 12 test bays on an east/west axis bounded on each end by a guard bay. The eastern six test bays are framed in steel, and the western six bays are framed in wood. Each half of the building contains a symmetrical mix of vented and unvented cathedral and attic roofing systems and is built above a heated basement. During the heating season, the entire building is maintained at a uniform temperature within ±0.9°F (±0.5 K) by a computer control system, and data are stored with an aggregation period of approximately 20 minutes. The thermal performance phenomenology of a vented attic and cathedral ceiling are analyzed via heat transfer and mass flux parameter correlations. Attic and cathedral ceiling roofing system relative thermal integrities are compared as a function of framing material and ventilation status. Within the preliminary context of the data reported, it appears that metal framing yields a lower thermal integrity than wood framing with particularly poor performance when applied to a vented cathedral ceiling. The ridge vent mass flux in ventilated attics and cathedral ceilings is shown by the data reported to be largely independent of roof configuration.

INTRODUCTION

The Cloquet Residential Research Facility (CRRF) was constructed in 1997 and is located near Cloquet, Minnesota, about 23 miles southwest of the southern tip of Lake Superior. The CRRF is designed as a test bed to evaluate the in-situ, long-term, cold-climate performance of various building products, including thermal insulation, siding, roofing materials, and footing construction systems. Because of its proximity to Lake Superior, the CRRF is subject to various lake effect weather phenomena, most importantly, an elevated snowfall. Similar test facilities also have been constructed in Illinois (Rose 1989) and Florida in order to determine performance under moderate and warm climatic conditions, respectively.

The CRRF is equipped with a computerized data acquisition and control system that captures and records measurements from several hundred transducers while simultaneously controlling the building heating systems. The system is configured for remote operation and control. Recorded data are transmitted over the Internet to a remote server, while remote control is accomplished via a direct telephone connection. The data acquisition philosophy is based upon an accurate measurement of the building energy consumption, allowing the energy performance of the tested composite building envelope systems to be compared.

Data acquisition commenced on October 24, 1997, with a subset of the full transducer array. During the next four months, the monitored transducer count increased to reach a full complement of 400 on March 4, 1998. During this period, the envelope air leakage integrity was progressively tightened by sealing up instrumentation and power cable conduits, reaching the nominal design integrity (that is, the integrity achieved with all the designed sealing strategies implemented) on March 4 as well. The data reported here span the period from 3/4/98 to 4/17/98 and thus represent a preliminary evaluation of the CRRF attic and cathedral ceiling thermal

Louis F. Goldberg is a senior research associate in the College of Architecture and Landscape Architecture, University of Minnesota, Minneapolis. **Patrick H. Huelman** is an associate professor and **Barry B. Bridges** is a project engineer in the Department of Wood and Paper Science, University of Minnesota.

performance under nominal design and moderate winter weather conditions.

BUILDING DESCRIPTION

A schematic layout of the CRRF is given in Figure 1. The CRRF has a single story built upon a full basement, the most prevalent foundation type in Minnesota. The main floor of the CRRF is divided into 12 horizontal parts along the major east-west axis. The two central sections are further divided into two bays each along the north-south axis. This topology yields 12 test bays bounded on each end by a guard bay. The bays are numbered sequentially from west to east. The west basement is common to bays 1 through 6, with the east basement spanning bays 7 through 12. As noted in Figure 1, the guard bays embrace both the main floor and basement levels and are intended to thermally guard bays 1 and 12 and both east and west basements, allowing all the test bays to be subject to the same thermal boundary conditions on the partition walls. The test bays are all 10 ft (3.1 m) in width, while the guard bays are 12 ft (3.7 m) wide, yielding east and west basement test bays with a width of 50 ft (15.2 m) each.

The specifications of the envelope components in each of the main floor test and guard bays are given in Table 1. For the purposes of this discussion, attention may be focused on the ceiling and attic configurations. The western four test bays (1 through 4) are equipped with a wood truss roof structure, while the eastern 4 bays (9 through 12) have a metal frame roof structure. These east and west test bay groups are symmetrical in layout about the central north-south axis (between bays 5 and 7). The west guard bay and bays 1 and 2 form the attic test bay group, with the ventilated bay 1 bounded by the unventilated west guard bay and bay 2. Bays 3 and 4 have cathedral ceilings, with the former vented and the latter unvented. Thus, symmetrically, bays 9 and 10 have cathedral ceilings with the former unvented and the latter vented. The east guard bay and bays 11 and 12 form the metal side attic test bay group, with the vented bay 12 bounded by the unvented bay 11 and east guard bay.

Bays 1 through 4 and 9 through 12 share a common full roof structure with both north- and south-facing slopes, while the center four bays (5 through 8) each have a half-roof structure with a south-facing exposure on bays 6 and 8 and a north-facing exposure on bays 5 and 7. Further, in order to accommodate the 11 ft (3.4 m) protrusion of bays 6 and 8 on the south side of the building, the ridge line above these bays is elevated above that of the remaining bays and is displaced south of the building centerline to a location above the east/west partition separating bays 5 and 7 from bays 6 and 8. Thus, the roof chord length is longer for the center four bays than the other bays. In order to maintain the envelope configuration similarity necessary for valid envelope energy performance comparisons, the data discussed focus on bays 1 through 4 and 9 through 12. The ceiling/attic insulation installations are symmetric around the central north/south axis on the wood and metal bays, while the vented and unvented attics share the same insulation. Within each metal and wood test group, the cathedral ceilings have BIBS insulation and the attics have IS-III insulation (see Table 1 for nomenclature). The nominal design RSI value of the IS-III insulation in the attics is R-38 ($ft^2 \cdot h \cdot °F$)/Btu (6.7 ($m^2 \cdot K$)/W), that of the BIBS insulation in the vented cathedral ceilings

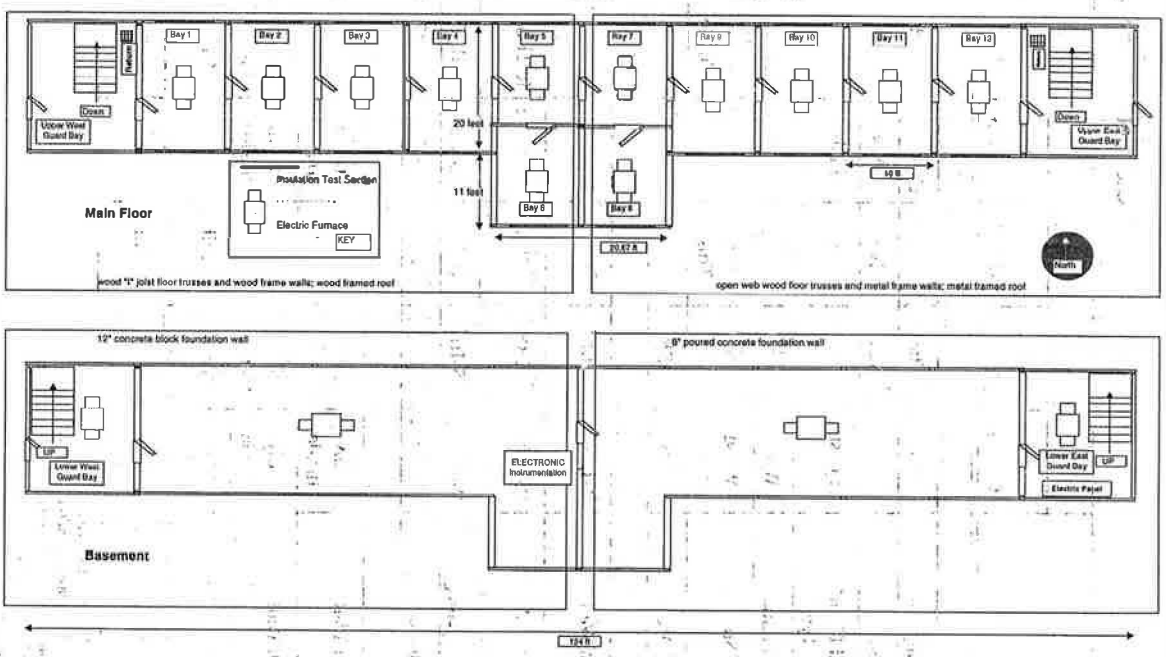

Figure 1 *Cloquet Residential Research Facility layout schematic.*

BACK TO PAGE ONE

TABLE 1
Cloquet Residential Research Facility Bay Specifications

	Bay Designation												
	West Guard	Test 1	Test 2	Test 3	Test 4	Test 5	Test 6	Test 7	Test 8	Test 9	Test 10	Test 11	Test 12	East Guard
Construction														
Ceiling	Flat	Flat	Flat	Cathedral	Cathedral	Cathedral	Flat	Cathedral	Flat	Cathedral	Cathedral	Flat	Flat	Flat
Vented?	No	Yes	No	Yes	No	No	No	Yes	Yes	No	Yes	No	Yes	No
Wood Floor[4] Truss Type	I joist	I joist	I joist	I joist	I joist	I joist	I joist	Open Web	Open Web	Open Web	Open Web	Open Web	Open Web	Open Web
Wall Frame	Wood	Wood	Wood	Wood	Wood	Wood	Wood	Metal	Metal	Metal	Metal	Metal	Metal	Metal
Roof Structure	Wood Truss	Wood Truss	Wood Truss	Wood Frame	Wood Frame	Wood Frame	Wood Frame	Metal Frame	Metal Frame	Metal Frame	Metal Frame	Metal Truss	Metal Truss	Wood Truss
Roof Deck	OSB[5]	OSB	OSB	OSB	OSB	OSB	OSB	OSB	OSB	OSB	OSB	OSB	OSB	OSB
Insulation[3]														
North Wall	R-15 batt	BIBS[1]	BIBS	Cellulose	R-21 batt	BIBS	R-13 batt (non-test)	BIBS	R-13 batt (non-test)	R-21 batt	Cellulose	BIBS	BIBS	R-15 batt
South Wall	R-15 batt	BIBS	BIBS	Cellulose	R-21 batt	R-13 batt (non-test)	BIBS	R-13 batt (non-test)	BIBS	R-21 batt	Cellulose	BIBS	BIBS	R-15 batt
North Ceiling	R-38 batt	IS-III[2]	IS-III	BIBS	BIBS	BIBS	n/a	BIBS	n/a	BIBS	BIBS	IS-III	IS-III	R-38 batt
South Ceiling	R-38 batt	IS-III	IS-III	BIBS	BIBS	n/a	R-38 batt	n/a	R-38 batt	BIBS	BIBS	IS-III	IS-III	R-38 batt
Vapor Retarder														
North Wall	Poly Inside	6 Mil Outside	6 Mil Inside	6 Mil Inside	6 Mil Inside	None	Non-Test	None	Non-Test	6 Mil Inside	Kraft Inside	6 Mil Inside	6 Mil Outside	Poly Inside
South Wall	Poly Inside	6 Mil Outside	6 Mil Inside	6 Mil Inside	6 Mil Inside	Non-Test	None	Non-Test	None	6 Mil Inside	Kraft Inside	6 Mil Inside	6 Mil Outside	Poly Inside
North Ceiling	Poly Inside	6 Mil	6 Mil	None	6 Mil	Inside	n/a	6 Mil	n/a	6 Mil	None	6 Mil	6 Mil	Poly Inside
South Ceiling	Poly Inside	6 Mil	6 Mil	None	6 Mil	n/a	Inside	n/a	Inside	6 Mil	None	6 Mil	6 Mil	Poly Inside

1. Blown in blanket system.
2. Loose fiberglass insulation mixed with glue.
3. Non-test partition wall insulation: R-13 batt.
4. Bay floor insulation: R-38 encapsulated batt.
5. Oriented strand board.

(bays 3 and 10) is R-32 (RSI 5.6), and that of the BIBS insulation in the unvented cathedral ceilings (bays 4 and 9) is R-36 (RSI 6.3). Hence, these differences in nominal insulation thermal resistance need to be considered in evaluating the energy performance data. Vapor retarders are installed in all eight bays under consideration, with polyethylene sheeting used in all bays except the vented cathedral ceilings (bays 3 and 10).

The vented cathedral ceilings are fitted with polystyrene baffles extending from the soffits to within 10 in. (25 cm) of the ridge vent, while the vented attics have similar baffles extending from the soffits about one-third of the way up the roof line. Care was taken to seal the partitions between vented and unvented bays as completely as possible, with extensive use of gaskets, tape, and sealants.

INSTRUMENTATION AND CONTROL

The design of the instrumentation is based on the philosophy of accurately monitoring the energy consumption within each bay, allowing rigorous whole bay envelope thermal performance comparisons to be made. Central to this objective is the need to maintain the bay set-point temperatures as close to a uniform value as possible. Hence, the design control band was set at ±0.9°F (±0.5 K) to be realized in all 16 heated bays (12 test, 2 guard, and 2 basement) simultaneously. To this end, a symmetric dual-processor computer running a multi-tasking operating system is configured with dual instrumentation busses and dual 16-bit analog-to-digital converters. One of these busses is devoted to control of the heating systems, while the other gathers data from the building transducers. The busses operate independently so that in the event of a power or software failure, the control function continues to operate even though the data capture may have ceased. All 16 heating units are under the direct digital control of the central computer, enabling complete flexibility in control parameter/actuator coupling. Bay temperatures are determined as the electrical average of two copper-constantan thermocouples located 12 in. (30.5 cm) away from the center of the north and south exterior walls. The measurement precision of the thermocouples is 0.2°F (0.1 K) with a noise amplitude an order of magnitude smaller. Under full-load conditions (simultaneous control, data capture, and Internet communication), the central computer maintains a control cycle time better than four seconds on all 16 heating units simultaneously.

As the CRRF is electrically heated, the energy consumption of each bay is monitored with a standard watt-hour meter fitted with an optical pulse initiator yielding a sensitivity of 72 watt-hours per counted pulse. Pulses are accumulated using independent solid-state counters, thus ensuring an accurate count. The temperature and mass flux data presented are measured with copper-constantan (type-T) thermocouples and hot wire anemometers, respectively. The precision of the thermocouple measurements is the same as that of the bay temperatures discussed above. Ridge vent mass fluxes in each of the vented bays are monitored with hot wire anemometers, each transducer having an individual, multi-point NIST-traceable calibration of 0 ft/s to 4.9 ft/s at 32°F (0 m/s to 1.5 m/s at 0°C). These transducers have a process operating temperature range of –40°F to 392°F (–40°C to 200°C) with a quoted 2% accuracy and are considered to be reliable for the extreme temperature range encountered at the CRRF. Each transducer sensing element is located at the geometric center of the ridge vent and thus measures the mass flux at that point only. Thus, the area-integrated mass flow through each ridge vent cannot be inferred from these data without recourse to computational fluid dynamics simulation.

Over the course of the monitoring period described here, all the bays in the CRRF have been maintained at a set-point temperature of 68°F (20°C). Over this period, data have been aggregated over a nominal 20 minute interval prior to being stored. Each aggregation period includes six or seven data scans of the noncontrol parameter transducers, allowing a sufficient period between scans for the capture of transient effects on selected transducers if desired. The data are stored in quadruplicate in three separate locations using three different media to ensure security.

RESULTS

The results are presented here in three sections. The first describes the phenomenology (or physical behavior) observed for wood-framed bays with a vented attic and a cathedral ceiling. The second section describes the relative thermal integrity of the four vented and four unvented bays with full roofs, and the last section deals with the observed ridge vent mass fluxes.

Vented Attic and Cathedral Ceiling Phenomenology

The phenomenological behavior of a vented attic as observed at the CRRF for bay 1 is shown in Figure 2. In order to maintain legibility of the scatter plots shown, only 1 in 15 recorded data points is plotted, although the statistics are performed on all the data points. The data reported are collected on a north-south oriented vertical plane located at the center of the bay. Proceeding from left to right and top to bottom, the data show strong correlations between the mean attic temperature (MAT) and the mean inlet temperature of the north and south soffits (Figure 2a) as well as between the MAT and the outlet temperature at the ridge vent (Figure 2b) as may be expected. No correlation between the inlet/ridge temperature difference and the MAT is apparent (Figure 2c), nor does this temperature difference correlate with the temporal MAT gradient (not plotted). Considering the ridge mass flux in Figure 2d, this also is observed to be independent of the MAT, suggesting that thermally induced buoyancy effects are not significant within the measurement precision. Also notable is the small magnitude of the recorded mass flux, with a mode value of 0.02 lb/(ft^2·s) (0.1 kg/(m^2·s)) or less. At the prevailing temperatures, the air density is typically in the range of 0.07 lb/ft^3 to 0.08 lb/ft^3 (1.2 kg/m^3 to 1.3 kg/m^3), implying a small mode air velocity at the ridge of about 0.26 ft/s (0.08 m/s). It should be noted that at these low velocities, measuring the

BACK TO PAGE ONE

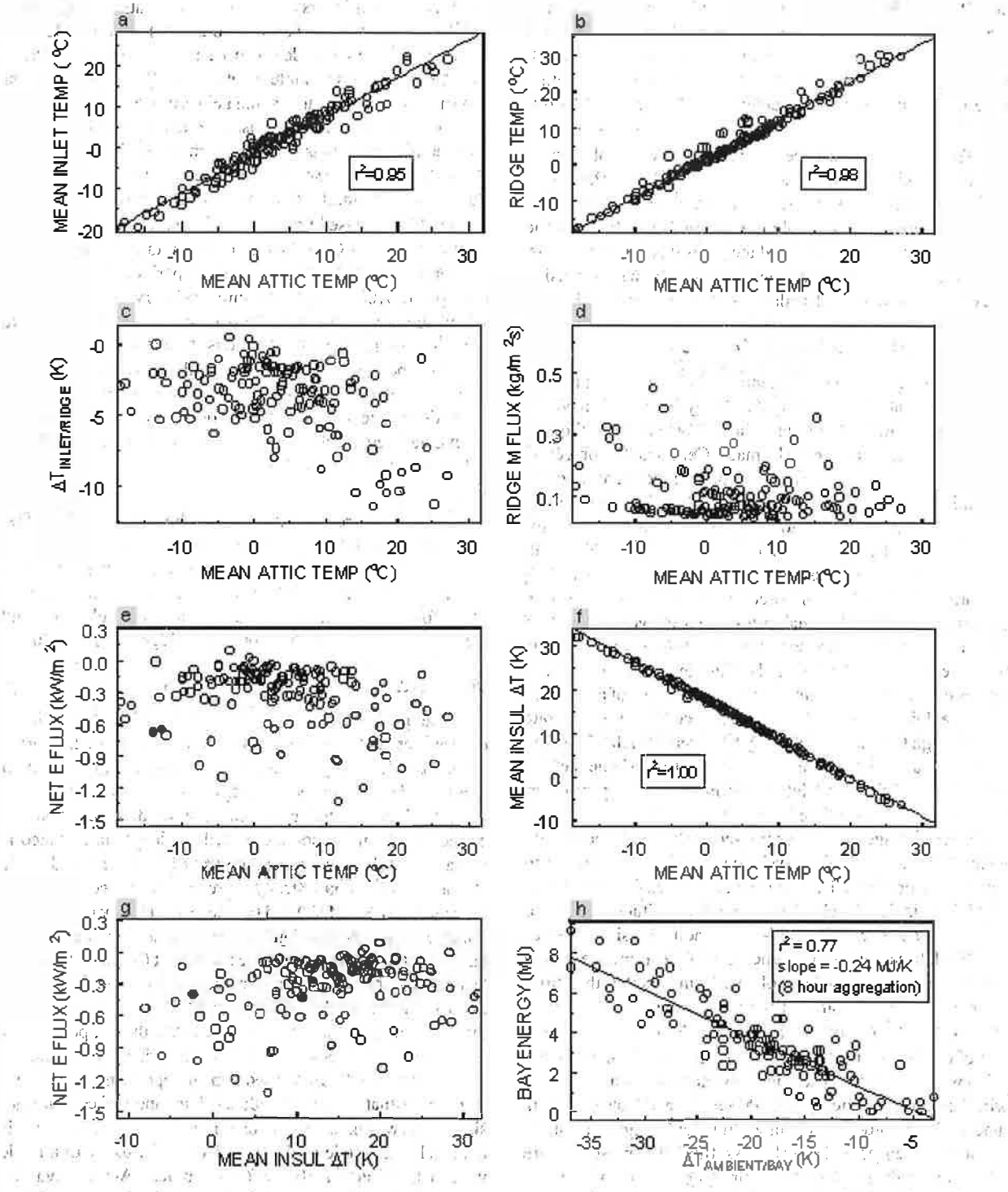

Figure 2 *Vented attic phenomenological behavior (bay 1).*

resultant pressure differentials on the order of 0.002 in. of water (0.5 Pa), is problematic. Thus, even though these measurements are being recorded, they are not considered to be reliable at this stage because the measurements are within the zero point calibration hysteresis of the transducers themselves. If sufficient funding becomes available, it may be possible to correct this problem with the installation of a dynamic auto-zeroing system. Nevertheless, the raw temperature data recorded indicate that no instance of flow reversal (entry at the ridge, exhaust at the soffit) occurred.

Combining the inlet/ridge temperature with the mass flux yields the net attic air enthalpy flux, which does not correlate with the MAT (Figure 2e). As Figure 2e is a combination of Figures 2c and 2d, neither of which correlate with the MAT individually, this lack of correlation is expected. The mean temperature difference nominally is perfectly correlated with the MAT as a result of the temporally uniform temperature maintained within the bay, as shown in Figure 2f. Plotting the mean temperature difference across the ceiling insulation against the net attic enthalpy flux in Figure 2g also shows the absence of a significant correlation. As the plot is performed for contemporaneous data, it follows that introducing a phase delay between the insulation temperature difference and net enthalpy flux may improve the correlation. This would account for air circulation and boundary layer effects within the attic cavity.

Finally, the net bay energy consumption is plotted against the ambient/bay temperature difference in Figure 2h. This provides a measure of the overall thermal integrity of the bay envelope as measured by the slope of the line (Goldberg 1984). A critical parameter in establishing this correlation is the size of the aggregation bin, which is strongly dependent on the envelope construction. For example, envelopes with a large earth-contact coupling can have bin sizes as large as two days, while closely coupled envelopes have bin sizes closer to half a day. The uniformity and constancy of the internal temperature is also important, with better control yielding smaller bin sizes. Thus, a bin size of eight hours yields a correlation coefficient (r^2) of 0.77, which is reasonable for the CRRF system configuration.

The phenomenology of a vented cathedral ceiling is shown for bay 3 in Figure 3. Figure 3a gives the correlation between the temperature of the south air vent baffle casing measured on the insulation side (BWT) and the mean baffle air temperature (BAT) computed as the average of the measured inlet and ridge temperatures. A linear correlation of these parameters yields an r^2 of 0.88, only marginally worse than the quadratic correlation r^2 of 0.91 shown. While the correlation is certainly linear for BWTs below 59°F (15°C) where the scatter is reduced, at higher temperatures the scatter is increased and statistically a quadratic fit appears better. This may, however, be an effect of the relative paucity of higher temperature data, which will become apparent as warm temperature data are accumulated over the course of the experiment. The same arguments also apply to Figures 3b and 3c where the correlation with the ridge temperature appears to be better than the correlation with the inlet temperature at the soffit. Figure 3d depicts the correlation between the BWT and the inlet/ridge temperature difference. Arguably, in this case, a quadratic fit, while yielding a statistically better correlation than a linear fit, is not physically reasonable since an increase in baffle wall temperature cannot produce a decrease in advected air temperature difference magnitude at low temperatures, as shown in Figure 2d for BWTs less than 32°F (0°C). However, it is significant that, given the correlation of Figure 3a, the advected temperature difference is correlated with the BWT, unlike the corresponding case in the attic (Figure 2c). Figure 3e also shows a lack of correlation between ridge mass flux and the BAT in agreement with Figure 2d for an attic. Thus, it appears that even in the context of a closer thermal coupling between the thermal flux entering the baffle cavity and the net baffle enthalpy flux (Figures 3d and 3g), buoyancy effects are not of major significance in determining the magnitude of the ridge mass flux. The significance of Figure 3g is perhaps most evident by comparing it with Figure 2g for an attic. The correlation between the insulation temperature difference and net enthalpy flux exists statistically (a linear correlation yields an r^2 of 0.52 compared with 0.60 for a quadratic correlation). This shows that the heat flux entering the baffle cavity from the bay is more closely coupled temporally to the advective flux, unlike the attic situation. This confirms a theoretically expected heat transfer result in which a baffled vented cathedral ceiling behaves more like a duct than a vented attic.

Finally, the overall bay thermal integrity is shown in Figure 3h. Compared with Figure 2h, the reduced overall envelope thermal integrity of a bay with a vented cathedral ceiling is evident. With similar r^2 values, Figure 3h yields a slope of –174 Btu/°F (–.33 MJ/K) for a vented cathedral ceiling compared with –126 Btu/°F (–.24 MJ/K) for a vented attic (the smaller the slope magnitude, the higher the envelope integrity). Clearly, as these values reflect the integrity of the entire externally exposed bay envelope, part of the difference can be ascribed to differences between the BIBS and the cellulose wall insulation used in bays 1 and 3 (Table 1). However, it is anticipated that further analysis of the experimental data will confirm that these differences are small in comparison with the larger effect produced by the difference in roof system configuration.

Attic and Cathedral Ceiling Relative Thermal Integrity

The thermal integrity results are developed on the basis of a continuum mechanics analysis of building energy consumption (Goldberg et al. 1984, appendix C). The result of this analysis yields the following model for determining the energy performance of a building envelope:

$$E_{aux} - K_{wh}E_{wh} = \bar{g}(\bar{T} - T_e) + Q^* \qquad (1)$$

BACK TO PAGE ONE

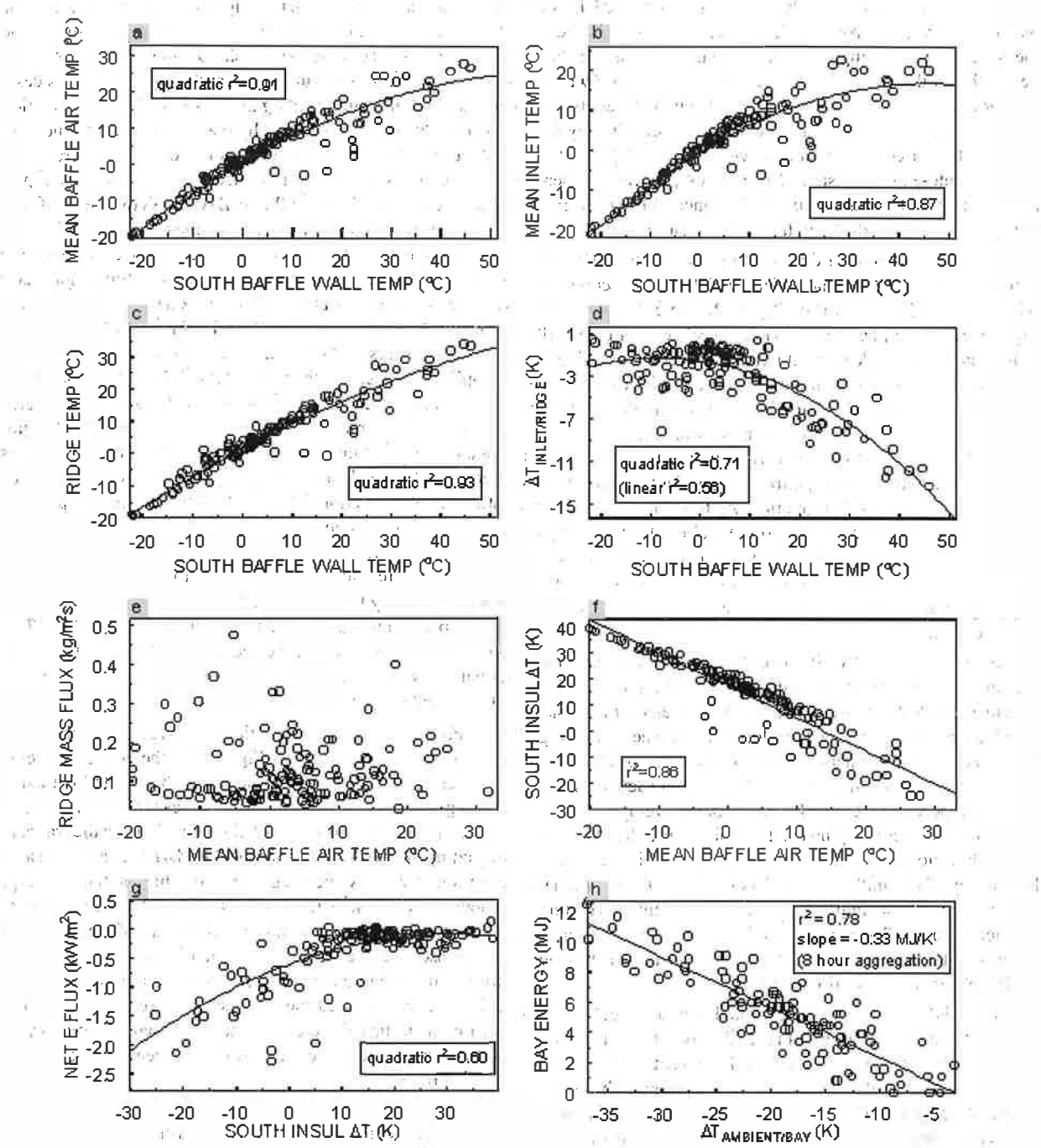

Figure 3 *Vented cathedral ceiling phenomenological behavior (bay 3).*

where

E_{aux} = net auxiliary energy input through the building envelope from all relevant sources (for example, electricity, gas, wood);

K_{wh} = water heater loss coefficient representing the amount of energy supplied to the water heater that is unavailable for space heating owing to gray water loss;

E_{wh} = water heater energy input;

$\bar{g}$ = time-averaged transport function (advection and diffusion);

$\bar{T}$ = volume-averaged internal temperature;

T_e = external temperature (either ambient or adjoining unheated space);

Q^* = integration constant minus the total control volume heat gain independent of the interior/exterior temperature difference (typically solar plus occupants).

In the case of the CRRF, E_{wh} is zero and Q^* is just the integration constant, so a plot of the temperature difference vs. E_{aux} yields a slope representing $\bar{g}$, or the envelope thermal integrity. Now, from the analysis on which Equation 1 is based, $\bar{g}(\bar{T}-T_e)$ represents the surface area integral of the energy transport fluxes on the control volume surface. Thus, isolating the temperature difference for a particular envelope component (when a discrete difference is measured) and correlating that against the whole bay energy consumption shows the extent to which the thermal integrity of that particular component influences the whole bay energy consumption. In other words, this yields a purely phenomenological indication of whether the thermal integrity of a particular component is physically related to the energy consumption plus a relative indication of the magnitude of the relationship. No information on the relative magnitudes of the components of $\bar{g}$, whether diffusion (thermal conduction) or advection (infiltration), is provided; neither can the mechanisms by which the envelope configuration influences the diffusion and advection components be extracted.

Thus, noting that $\bar{T}$ is essentially constant (variability of ±0.9°F [(±0.5K]), plotting the net bay energy consumption against the relevant T_e enables the physical connection between the roof system configuration and the bay energy consumption to be revealed. In particular, T_e is represented by the mean attic air temperature (MAT) in Figure 4 for the attics and by the mean baffle air temperature (BAT) or interior deck temperature in Figure 5 for the cathedral ceilings. As noted above, while such a correlation does not yield the absolute thermal integrity of the roof system in isolation, it does enable the relative integrity of the test bays with the same exposed external envelope areas to be compared as a function of the roof system configurations. Thus, provided the correlation

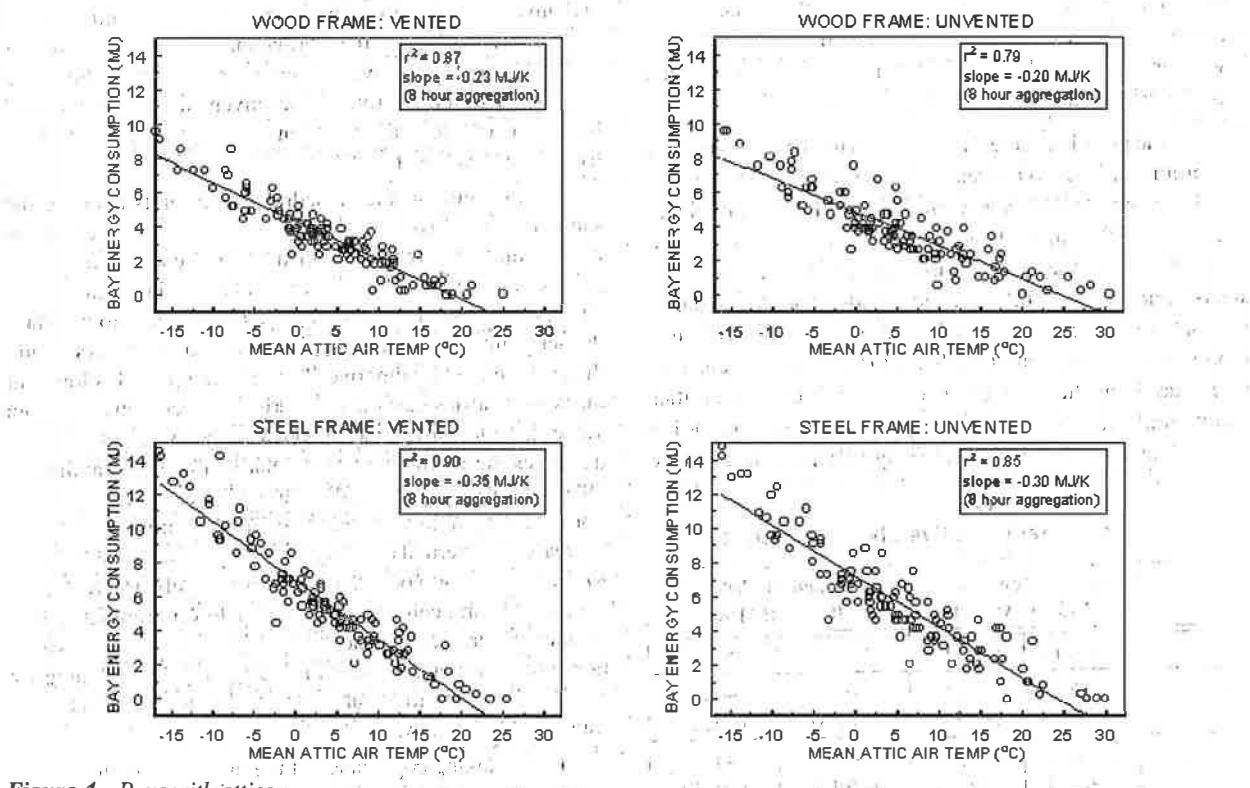

Figure 4 Bays with attics.

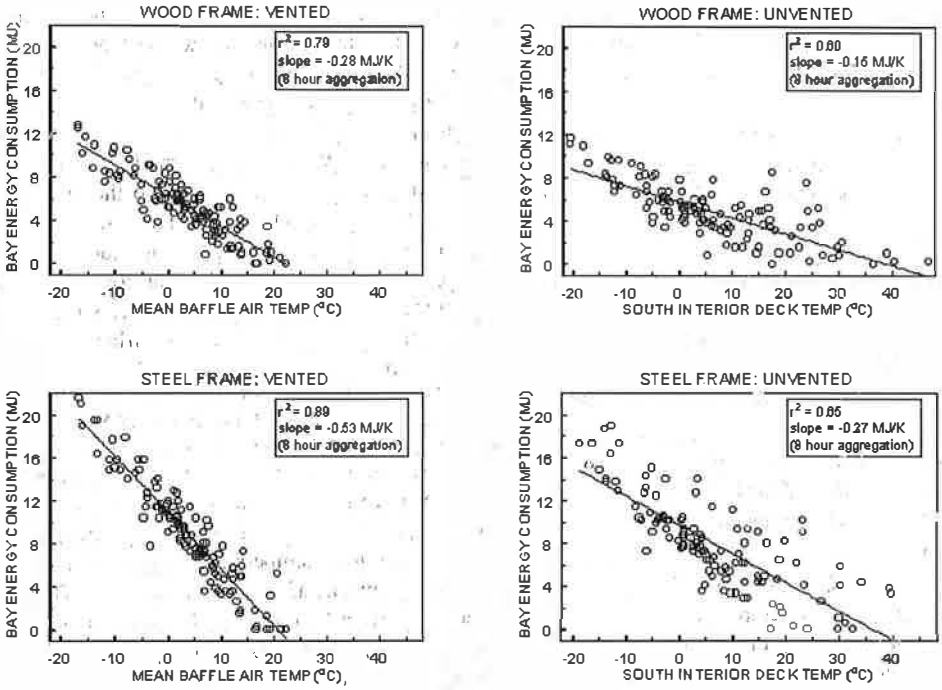

Figure 5 *Bays with cathedral ceilings.*

coefficient produced by a linear regression performed on the data is statistically significant, the gradient of the line gives a relative measure of the thermal integrity of the roof system. These gradients are extracted from Figures 4 and 5 and summarized in Table 2.

All the plots in Figure 4 are shown with the same abscissa and ordinate scales so the relative slopes of the linear regression lines are apparent. The correlation coefficients in Figure 4 range from 0.79 to 0.90, indicating a statistically significant correlation in all cases. Comparing the ordinate range of the steel-framed bays to those of the wood-framed bays shows that on a whole bay envelope basis, the steel bays consume more energy to maintain the 68°F (20°C) set-point temperature. Examining the ordinate range shows that the vented attics maintain a colder average air temperature over the reporting period than the unvented attics, as may be expected. Referring to Table 2, a comparison of the symmetric wood/steel vented and unvented attic pairs shows that relative to wood framing, steel framing decreases the thermal integrity by 52% and 50% for the vented and unvented cases, respectively. For each framing material, relative to the unvented bays, the vented bays yield a decreased thermal integrity of 15% and 17% relative to the unvented bays.

TABLE 2
Roofing System Relative Thermal Integrity

	Attic Btu/°F (MJ/K)		Cathedral Ceiling Btu/°F (MJ/K)	
Frame	Wood	Steel	Wood	Steel
Vented	−121 (−0.23)	−184 (−0.35)	−147 (−0.28)	−279 (−0.53)
Unvented	−105 (−0.20)	−158 (−0.30)	−79 (−0.15)	−142 (−0.27)

As in Figure 4, the cathedral ceiling plots also use the same abscissa and ordinate scales. The correlation coefficients range from 0.60 to 0.89, with the lower coefficients being produced in the unvented bay regressions. As in the case of the attics, the steel-framed bays require more energy to maintain the set-point temperature than the wood-framed bays, while the average temperature over the reporting period is lower in the vented baffles than on the interior roof deck surface. From Table 2, comparing the wood/steel pairs, steel framing decreases the thermal integrity relative to wood framing by 89% and 80% for the vented and unvented cases, respectively. For each framing material, ceiling venting nominally decreases the thermal integrity relative to the unvented case by 87% and 96% for wood and steel, respectively. However, the vented cathedral ceilings have an 11% lower nominal ceiling insulation thermal resistance, reducing, to a rough approximation (given the correlation of Figure 3g), the thermal integrity penalty of venting to about 76% and 85% for wood and steel framing, respectively.

Lastly, taking cognizance of the difference in the insulation thermal resistances, a comparison between paired attics

BACK TO PAGE ONE

and cathedral ceilings (that is, same framing material and venting configuration) shows that in the vented situation, the cathedral ceiling reduces the thermal integrity relative to the attic by 22% and 51% for wood and steel, respectively. Again, to a rough approximation, factoring out the 16% decrease in insulation thermal resistance available in the cathedral ceilings, it appears that the thermal integrity penalty of the cathedral ceiling configuration itself declines to the vicinity of 6% and 29% for wood and steel, respectively. Thus, combined with the previous comparisons, this shows the relatively large energy penalty invoked when using steel framing for a ventilated cathedral ceiling. However, comparing paired *unvented* attics and cathedral ceilings yields an unexpected result, namely, that relative to the unvented cathedral ceilings, the unvented attics show a *reduced* thermal integrity of 33% and 11% for wood and steel, respectively. This is clearly counterintuitive given that the attics have a 6% greater insulation thermal resistance than the cathedral ceilings and that the data within the attic and cathedral ceiling groups are consistent without exception. A likely explanation for this is a systematic effect produced by using the south deck interior temperature as the abscissa in the unvented cathedral ceiling correlations, as indicated by the comparatively low r^2 regression values produced. This temperature was chosen for its geometric compatibility with the corresponding baffle or attic air temperatures (that is, all within the roof deck envelope boundary). However, from a heat transfer perspective, using the temperature recorded between the shingles and the roof deck may be a better choice for the unventilated cathedral ceilings. Further examination of these shingle/roof deck temperature data, as well as other available data including bay ceiling heat fluxes and bay wall temperatures, will be required before this apparent anomaly can be clarified further.

As noted above, the correlation data do not allow the results to be explained in terms of the transport function components. It could be argued, for instance, that the smaller relative thermal integrity of the steel bays is a result of increased infiltration in these bays. This may very well be the case caused by, for example, the inability to seal a polyethylene vapor retarder to a metal stud as effectively as to a wooden stud. However, whatever the composition of the transport function, the data do show that the thermal integrities of the roof systems monitored are physically linked to the whole bay energy consumption with various magnitudes of linkage depending on the roof system configuration.

Ridge Vent Mass Flux

The time series ridge mass flux sensor profiles are given in Figure 6. With the exception of bay 1, the mass fluxes are recorded at the middle of the center truss or beam cavity in each bay. In bay 1, data are available during the reporting period for the center cavity as well as the adjacent cavity to the east. Note that the linear discontinuities in the profiles at about 80 hours and 400 hours indicate the occurrence of power failures.

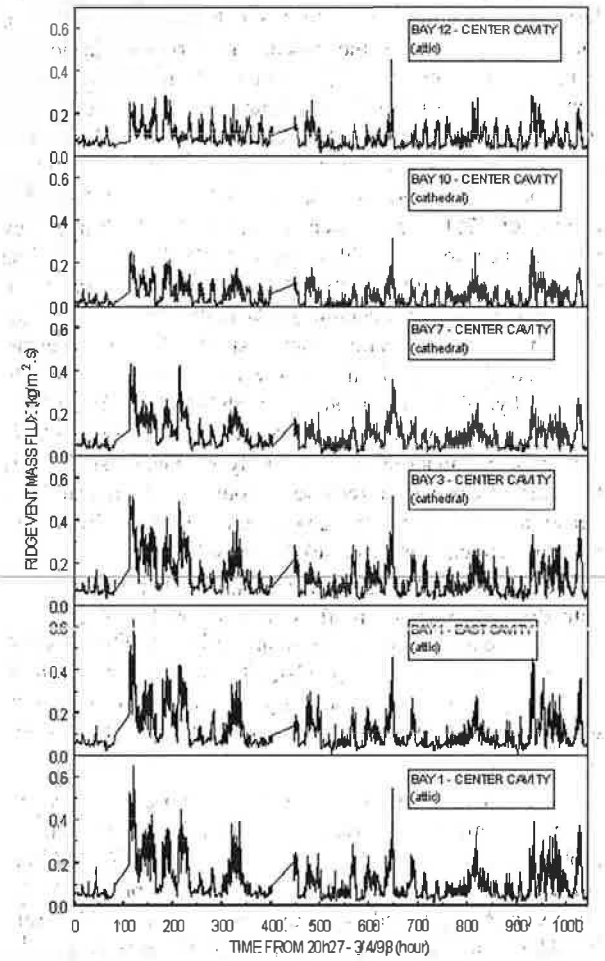

Figure 6 *Ridge vent mass flux time profiles.*

The center and east cavity profiles in bay 1 are very well correlated both with respect to phase and peak magnitude, indicating no visible evidence of recirculation within the ridge vent. Further, the peak events are well correlated in time for all five ventilated bays shown, while the peak magnitudes decline uniformly from west to east moving from bay 1 to bay 10 prior to increasing marginally in bay 12. Note that bay 7 (with a half-, north-facing roof, and increased stack effect owing to a longer roof chord length) is included in this comparison to emphasize the observation that the ridge mass fluxes appear to be largely independent of the roof configuration, as anticipated by the results noted above. Assuming that the mass flux calibrations have not drifted (which could account for the differences in magnitude but not the similarity in phase—however, one would expect such a drift to show up in bay 1 as well, which is not the case), then these data suggest that factors other than roof configuration require investigation as possible explanations for the observations.

BACK TO PAGE ONE

DISCUSSION

The principal result from the preliminary data analysis discussed is that steel-framed roofing systems appear to be less energy-efficient than their wood-framed counterparts. Vented, steel-framed cathedral ceilings perform significantly worse than all the other configurations discussed, the smallest penalty being a factor of 1.5 compared to a steel-framed vented attic. Vented attics and cathedral ceilings are not as energy-efficient as their unvented counterparts, but the venting penalty for cathedral ceilings is more than that for attics by a factor of 1.7. In the vented case, attics yield superior energy performance to cathedral ceilings, partly because of the greater insulation thermal resistance installed in the attics. In the unvented case, the data imply the counterintuitive conclusion that cathedral ceilings yield superior thermal performance to attics. This is most likely a systematic effect rather than a physical reality, requiring further investigation for its explanation. However, it needs to be emphasized that these inferences are made within the purely thermal perspective of the data presented. Inferences about the overall relative performance of the roofing systems monitored (including moisture effects, for example) are not warranted.

The heat and mass transfer characteristics of vented cathedral ceilings with baffles are confirmed to be different from those prevailing in ventilated attics, as theoretically expected. The former exhibit advective heat transfer behavior akin to a duct, while the latter arguably function as cavities with all the attendant effects of flow circulation and turbulence.

The ridge vent mass fluxes observed are very small in magnitude, making the measurement of pressure differentials problematic. Thus, the pressure differential data recorded are considered to be too unreliable for use until the pressure transducers can be equipped with a dynamic auto-zeroing capability. The data also show to a first approximation that the recorded mass fluxes are not dependent on the roof configuration and are not influenced by thermally induced buoyancy effects.

CONCLUSIONS

Given the preliminary nature of the data, restricted as they are to a six-week period in March and the first half of April, the drawing of any definite conclusions is not warranted. Further, as the data discussed only refer to aspects of the thermal performance, these data cannot be used to infer the overall relative performance of any of the roofing systems monitored, particularly with respect to issues such as moisture control and ice dam prevention. However, within these limitations, the following tentative assessments may be made:

1. Steel-framed cathedral ceilings and attics show a lower envelope thermal integrity than their wood-framed counterparts.
2. Steel-framed vented cathedral ceilings so far have produced the lowest thermal integrity of the systems discussed, suggesting that steel framing as implemented at the CRRF may not be appropriate for use in ventilated cathedral ceilings.
3. Unvented attics and cathedral ceilings show a higher thermal integrity than their vented counterparts, but the venting penalty seems to be smaller for attics than for cathedral ceilings.
4. Vented attics appear to perform better than vented cathedral ceilings for the same framing type.
5. Within the temporal and climatic limits of the analyzed data set, ridge mass fluxes in vented attics and cathedral ceilings show first-order independence from roof configuration as implemented at the CRRF.
6. Thermally induced buoyancy effects do not appear to be a primary influence on the ridge mass flux in vented attics and cathedral ceilings.

ACKNOWLEDGMENTS

The CRRF was built and is operated under the sponsorship of the CertainTeed Corporation. While the authors gratefully acknowledge this support, they accept full responsibility for the contents herein.

Additional support for the preparation of this paper has been provided by Lofrango Engineering.

REFERENCES

Goldberg, L.F. 1984. A comparative experimental evaluation of five earth-sheltered houses. *Underground Space*, vol. 8, pp. 36-43.

Goldberg, L.F., R.L. Sterling, and J. Carmody. 1984. Solar/earth-sheltered housing demonstration project: Energy performance monitoring and results. Report prepared for the Minnesota Housing Finance Agency, Underground Space Center, University of Minnesota.

Rose, W.B. 1989. Research plan, configuration and instrumentation for the measurement of residential attic performance. Report delivered to ASTM E-6.95, Denver, Colorado.

BIBLIOGRAPHY

Burch, D.M., and S.J. Treado. 1979. Ventilating residences and their attics for energy conservation—An experimental study. *Summer Attic and Whole House Ventilation*, M.H. Rappert, ed. Washington, D.C.: National Bureau of Standards.

Forest, T.W., and I.S. Walker. 1993. *Attic ventilation and moisture.* Ottawa: Canada Mortgage and Housing Corporation.

Peavey, B.A. 1979. A model for predicting the thermal performance of ventilated attics. *Summer Attic and Whole House Ventilation*, M.H. Rappert, ed. Washington, D.C.: National Bureau of Standards.

Rose, W.B. 1995. The history of attic ventilation regulation and research. *Thermal Performance of the Exterior Envelopes of Buildings VI,* pp. 125-134. Atlanta: American Society of Heating, Refrigerating and Air-Conditioning Engineers, Inc.

Wetherington, T.I. 1979. Measurement of attic temperatures in Florida. *Summer Attic and Whole House Ventilation*, M.H. Rappert, ed. Washington, D.C.: National Bureau of Standards.